

## Accepted Manuscript

Title: Measuring and accounting for solar gains in steady state whole building heat loss measurements

Author: S.F. Stamp R. Lowe H. Altamirano-Medina

PII: S0378-7788(16)30907-0

DOI: <http://dx.doi.org/doi:10.1016/j.enbuild.2017.06.063>

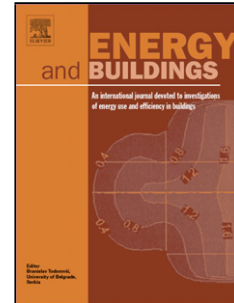
Reference: ENB 7726

To appear in: *ENB*

Received date: 21-9-2016

Revised date: 6-6-2017

Accepted date: 22-6-2017



Please cite this article as: S.F. Stamp, R. Lowe, H. Altamirano-Medina, Measuring and accounting for solar gains in steady state whole building heat loss measurements, *Energy & Buildings* (2017), <http://dx.doi.org/10.1016/j.enbuild.2017.06.063>

This is a PDF file of an unedited manuscript that has been accepted for publication. As a service to our customers we are providing this early version of the manuscript. The manuscript will undergo copyediting, typesetting, and review of the resulting proof before it is published in its final form. Please note that during the production process errors may be discovered which could affect the content, and all legal disclaimers that apply to the journal pertain.

# Measuring and accounting for solar gains in steady state whole building heat loss measurements

S.F. Stamp<sup>1</sup>, R., Lowe<sup>1</sup>, H. Altamirano-Medina<sup>1</sup>

## Abstract

To ensure good thermal performance is delivered consistently and at scale, there is a need to measure and understand the as-built heat loss of dwellings. Co-heating is a steady state, linear regression method, used to measure whole building heat transfer coefficients. This paper assesses the uncertainties in such outdoor, in situ, measurements due to the presence and treatment of solar gains. Uncertainties relating to solar gains are explored through both a number of field test results and simulated co-heating tests. Results demonstrate the potential for fractions of solar gains received on one day to be re-emitted on subsequent days. This dynamic behaviour can lead the steady state analysis to underestimate heat loss. Furthermore, inappropriate measurements of on-site solar radiation are shown to lead to bias in heat loss measurements. In particular, horizontal on-site solar radiation measurements are shown to significantly overestimate heat loss in buildings experiencing high proportions of direct gains through vertical openings. Both forms of uncertainty are dependent upon both the environmental test conditions and the characteristics of a test dwelling. Highly glazed, low heat loss and heavyweight buildings prove to be the most susceptible to such uncertainties, which ultimately limit both when tests can be successfully performed and which buildings can be tested.

## Keywords:

Outdoor testing, co-heating, heat loss coefficient, whole house heat loss, in-situ measurements, thermal performance, performance gap, uncertainty, solar gains.

## 1. Introduction

Addressing the performance gap, the difference between predicted and measured performance, has emerged as a key issue in reducing the energy demand and carbon emissions associated with the built environment [1, 2]. Studies that have specifically examined the thermal performance of the building fabric have provided evidence of a trend for higher than predicted measured heat loss among new builds [3, 4, 5, 6, 7] and of heat transfer mechanisms existing that significantly alter the performance of components and building envelopes [8, 9, 10]. Equally, the long assumed performance of traditional constructions have been called into question by recent field measurements, with lower than predicted U-values measured in both traditional stone and brick walls [11, 12, 13, 14].

Evidence suggests that this gap emerges through processes operating across all stages of the design and build process [15]. To reduce the risk of a gap in delivered performance undermining energy and carbon reduction policies, these processes need to be identified and understood to ensure good thermal performance is achieved in practice, on a consistent basis and at scale. Co-heating tests can provide measurements of the heat loss or transfer coefficient (HTC) of a dwelling [16], capturing the heat loss across the entire building envelope and as a result of multiple heat transfer mechanisms and interacting components. As such, the top-down, whole building heat loss measurement achieved by co-heating tests holds some alternatives

to, and advantages over, discrete measurements of single heat loss mechanisms (e.g. infiltration measurements [17]) or spot measurements (e.g. in situ U-value measurements [18]).

An understanding of heat loss reflecting the full build process is likely to require some degree of in-situ measurement of the thermal performance of conventional buildings in the field, and therefore within the outdoor environment. This inevitably reduces the degree of experimental control and presents a number of measurement challenges. In particular, this applies to the handling of solar radiation and the incorporation of solar gains into energy balance models. It is the uncertainty introduced by the presence of solar radiation in steady state co-heating measurements that this paper aims to address through three key aims:

- Identify the uncertainty within co-heating heat loss measurements associated with the presence of solar radiation.
- Characterise the resulting uncertainty and how it impacts heat loss measurements.
- Determine how these uncertainties can be addressed within the confines of the steady state method.

Before these aims are addressed, the co-heating methodology and its handling of solar gains is briefly reviewed.

*Email address:* samuel.stamp@ucl.ac.uk (S.F. Stamp)

## Nomenclature

$A_i$	Area of element $i$ ( $m^2$ )	$T_{si}$	Mean temperature of internal surfaces
$H$	Whole building heat transfer coefficient (W/K)	$U_i$	Thermal transmittance of element $i$ ( $W/m^2K$ )
$H_{meas}$	Measured heat transfer coefficient (W/K)	$\Delta T$	Temperature gradient ( $T_i - T_e$ )
$H_{true}$	Theoretical true heat transfer coefficient (W/K)	$D_{if}$	Diffuse solar radiation ( $W/m^2$ )
$Q_{elec}$	Electric heating power (W)	$D_{ir}$	Direct solar radiation ( $W/m^2$ )
$Q_{inf}$	Heat flow due to infiltration (W)	$G$	Global solar radiation ( $W/m^2$ )
$Q_{loss}$	Net heat flow across building envelop (W)	$HR$	Horizontally received solar radiation
$Q_{sol}$	Solar Gains (W)	$M$	Mean of all orientations
$R$	Solar aperture ( $m^2$ )	$N_{S,E,W}$	North, South, East, West facing
$S$	Incident solar radiation ( $W/m^2$ )	$NR$	Normally received orientated solar radiation
$T_e$	External air temperature	$V$	Vertically received solar radiation
$T_i$	Internal air temperature	$WM$	Weighted (by glazed area) mean of all orientations

## 2. Background: Co-heating method & solar gains

### 2.1. Co-heating method

As the total heat flow across the building fabric cannot be measured directly, the co-heating method uses a simplified energy balance equation to infer heat loss (equation 1). In an unoccupied dwelling, electric heating is used to provide constant and uniform mean elevated internal temperatures. This allows the adoption of a single zone model, reduces dynamic behaviour due to internal temperature variations and allows the heat input to be measured accurately through metering devices. To further limit the impact of dynamic behavior, tests are conducted over several days or weeks with data aggregated into 24 hours periods. Tests are then conducted under cold external conditions, typically between October and March in the UK [7]. The 'heat in' is then said to be equivalent to the 'heat loss' across this period (see figure 1, equations 1 - 3). The method then uses linear regression analysis to determine the building heat transfer or loss coefficient (HTC).

$$Q_{elec} + Q_{sol} = Q_{loss} \quad (1)$$

$$Q_{elec} + R \cdot S = H \cdot (T_i - T_e) \quad (2)$$

$$Q_{elec} = H \cdot \Delta T - R \cdot S \quad (3)$$

The method has origins in both the US [19, 20], where it was developed into the dynamic PSTAR method [21], and the UK [22, 23]. It is within the UK that the steady state, linear regression method formed an element of several key studies investigating building performance [24, 8, 25, 26, 4, 27] and helped identify the party wall bypass [8]. A protocol has been published in several iterations by researchers at Leeds Beckett University [28, 29, 30, 7], whilst a more comprehensive review of the method and its uncertainties can be found in Stamp [31].

### 2.2. Incorporating solar gains

Dependent upon both the test dwelling and the environmental conditions experienced during testing, solar gains can form a significant heat flow into the test dwelling. To avoid bias from their omission, they must be incorporated into co-heating analysis. As they cannot be measured directly, solar radiation is typically included either as an additional independent regression variable in multiple linear regression (MLR) with  $\Delta T$  and  $S$  as independent regression variables (equation 3) or used in a bi-axial regression (equation 4, see figures 3 and 7) as suggested initially by Palmiter [32] and used by Siviour [22]. Both methods yield very similar results [33, 34, 31], although the biaxial regression plot can provide a clearer visualisation of results.

$$\frac{Q_{elec}}{\Delta T} = -R \cdot \frac{S}{\Delta T} + H \quad (4)$$

Both these methods involve the creation of a further whole building parameter, the solar aperture, ( $R$  ( $m^2$ )), defined by its use within the regression process and the measurement of incident

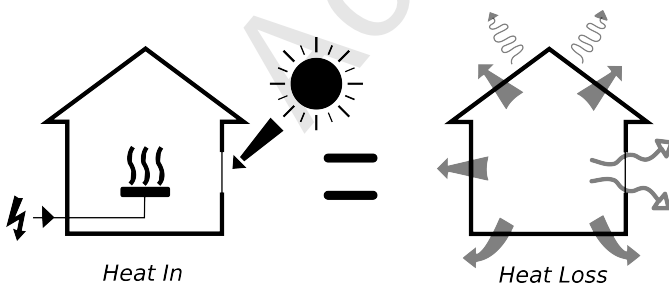


Figure 1: Co-heating test principal in which the heat in, consisting of electrical heat and solar gains, is equated to the total building heat loss, from convection, conduction and radiation across the entire building envelope.

solar radiation. The term  $R$  is well defined by Baker [34] who refers to the solar aperture as the ‘heat flow rate transmitted through the building envelope to the internal environment under steady state conditions, caused by solar radiation incident at the outside surface, divided by the intensity of incident solar radiation in the plane of the building ... It can be regarded as equivalent to a totally transparent area which lets in the same solar energy as the whole building’ [34, p.16].

Recent studies have shown a lack of consistency in both the measurement of solar radiation and the calculation of solar gains within the co-heating analysis (see table A.9). This has led to calls for clarity [35] and cast doubt over the reliability and consistency of the method [4, 36]. In particular the results of a recent field trial identified the need to understand how results are influenced by the measurement of solar radiation, the analysis techniques used and aggregation of data [35]. The true steady state nature of co-heating measurements has also been called into question, with Baker and van Dijk [37] having suggested for PASSYLINK test cells that 24 hour periods maybe insufficient (and as much as 10 day aggregation periods may be required), whilst previous work has suggested the potential for stored dynamics in co-heating tests [23, 38, 39].

Table A.9 also shows some tests in which solar gains were calculated numerically [see 40], using measured on site solar radiation along with assumed building and glazing properties to calculate solar gains [41, 16]. Recent work by the author has concluded this approach is unlikely to improve either range of suitable conditions for testing or the accuracy against statistical methods [31], with Bauwens and Roels [42] ‘strongly’ advising against this approach. Full uncertainty analysis regarding the assumptions and models used for such calculations must be reported alongside results.

### 2.3. Solar radiation incident upon a test dwelling

It is worth briefly considering the process in which incident solar radiation is converted into useful heat gains during a co-heating test. Solar radiation will be incident upon both the opaque and glazed elements of a test dwelling and will be made up of direct, diffuse and reflected components - the proportions of which become important when considering the type of solar radiation measurement made and used within the analysis. Radiation incident upon opaque surfaces will heat up those external surfaces, reducing the heat flow through the respective elements. Of that incident upon glazed elements, a fraction will be reflected, a fraction absorbed and then re-emitted by the glazing itself, and a fraction transmitted. The fraction transmitted into the internal space will subsequently be reflected or absorbed by the internal surfaces and furnishings before being re-emitted across a lagged response. This leaves a number of questions central to determining and incorporating solar gains into the steady state energy balance equation (equation 3):

- How much solar radiation is incident upon the test dwelling?
- How is it distributed across the building fabric and glazing?

- How much is therefore converted into useful internal heat gains?
- When is the heat absorbed from solar radiation emitted as gains to the internal space?

The first three questions relate to how well the measured, single and un-weighted value of  $S$  reflects the relationship between incident radiation and useful solar gains. The final question relates to how well the aggregated, static heat balance captures the dynamic behaviour of solar gains. These two issues are discussed in sections on the uncertainty related to stored solar heat gains (section 4) and the measurement of solar radiation (section 5). Proceeding these results, the research method used is described in the following section.

Whilst this paper therefore focuses upon understanding the uncertainties associated with solar radiation, it is important to acknowledge that these are not the only forms of uncertainty that may impact HTC estimates. Other sources may relate to equipment accuracies, experimental procedure (e.g. non-constant/non-uniform internal temperatures, party wall heat transfer, moisture loads), further environmental conditions (wind, sky temperatures) or the analysis method (e.g. attenuation bias, collinearity). Which uncertainties are present or dominate depends upon the test dwelling, environmental conditions, level of experimental control and analysis adopted. A broader review of the overall uncertainties can be found in Stamp [31], whilst it is those associated with solar radiation that fall within the scope of this paper.

## 3. Research Method

When assessing the uncertainties in this type of field test, the absence of knowledge regarding the ‘true’ value of a measured parameter can confound understanding - particularly of systematic errors and their drivers, as there is no reference between the true and measured values. Of course, the true value of a measurement can never be precisely know, but often when measuring the HTC of buildings, it is not only particularly hard to predict, but will also vary in unknown ways. This makes assessing the uncertainty within a measurement, or even a series of measurements, extremely difficult. Typical approaches for assessing systematic uncertainties involve adjusting single variables or by comparing sets of measurements [43]. However, in such field tests the external environment can neither be controlled nor replicated. Further, it remains difficult to separate out environmental variables or to systematically change building parameters.

For this research, a novel approach is adopted, in which co-heating tests have been simulated within the EnergyPlus simulation software [44]. Such an approach has been used to model a whole building undergoing co-heating tests [45, 31, 46] and upon both small test boxes [47] and single elements [48]. This simulated approach offers a number of advantages for understanding measurement uncertainties. Firstly, a true heat loss coefficient ( $H_{true}$ ) can be determined from both the inputs and

197 outputs of the simulation software and defined by the regres- 244  
 198 sion model (see equation 5)<sup>1</sup>. Comparing this true value ( $H_{true}$ ) 245  
 199 with the measured value ( $H_{meas}$ ) allows the assessment of both 246  
 200 systematic and random uncertainties. Secondly, both external  
 201 weather conditions and building parameters can be isolated and  
 202 changed on a one at a time basis - allowing identification of  
 203 the drivers for such uncertainties. Finally, equipment measure-  
 204 ment uncertainty is avoided, giving a clear picture of the testing  
 205 conditions and of environmental uncertainties.

$$H_{true} = \sum U \cdot A + \frac{\bar{Q}_{inf}}{\Delta T} \quad (5)$$

206 Here, the true value of the HTC is calculated from the U-  
 207 values ( $U$ ) and areas ( $A$ ) of each building element ( $i$ ), with ther-  
 208 mal bridges incorporated into elevated U-values. As the infil-  
 209 tration rate varies across this period, the average infiltration rate  
 210 ( $\bar{Q}_{inf}$ ) is divided by the mean temperature gradient across each  
 211 test period ( $\Delta T$ ).

212 Whilst they offer obvious advantages, a number of limita-  
 213 tions associated with simulated co-heating tests should be noted.  
 214 The simulated co-heating tests used here ignore sensor mea-  
 215 surement errors, simplified temperature distributions and sim-  
 216 plify heat loss pathways - ignoring complications associated  
 217 with workmanship (e.g. convective bypasses). However, here  
 218 they are used primarily to indicate the presence, potential scale  
 219 and drivers of systematic uncertainties. Results of field tests  
 220 are then used to identify further evidence of such uncertainties  
 221 within real co-heating tests.

### 222 3.1. Simulated co-heating tests

223 Simulated tests have been performed following the same  
 224 criteria as for field tests described in 2.1. This includes constant  
 225 electric heating, a uniform internal set-point (25°C), under con-  
 226 ditions of infiltration only (i.e. without ventilation). Ground  
 227 floor losses are directly coupled to the ground temperature, it-  
 228 self based upon monthly averages calculated in accordance with  
 229 ISO 13370:2007 [49]. Analysis is then conducted via MLR,  
 230 across 2 week periods.

### 231 3.2. Simulated test dwelling

232 For this work, a single detached building (tables 1 and 2) has  
 233 been simulated under a single weather file (Finningley TMY),  
 234 with a number of systematic changes then made the thermal  
 235 mass and glazing of the building (tables 3 and 4). Co-heating  
 236 conditions (as described in section 2.1) are adopted within the  
 237 simulations, run under either idealised steady state external con-  
 238 ditions or full weather files. The test building itself is con-  
 239 structed to modern fabric standards (notional UK building reg-  
 240 ulation standards [50]) and is modelled with a flat roof to avoid  
 241 uncertainty related to the presence of an unheated loft space  
 242 [31]. Glazing is split between two facades (see table 2) with the  
 243 orientation rotated between North-South and East-West axes in

<sup>1</sup>A non-intercept model is used here as an intercept model, although perhaps more elegant on a theoretical level, does not accurately describe either the losses coupled (gradient) or uncoupled (intercept) to  $\Delta T$

the analysis. Additionally, the construction is changed through  
 five thermal mass categories and a case with increased glazing  
 created. For consistency, in all cases the same HTC is main-  
 tained.

Table 1: Heat loss areas of simulated test dwelling

Element	U-value (W/m <sup>2</sup> K)	Area m <sup>2</sup>	W/K
Walls	0.18	116	20.8
Floor	0.13	42	5.5
Roof	0.13	42	5.5
Windows	1.4	13	18.2
Doors	1.0	1.4	1.4
Air Permeability	5 (m <sup>3</sup> /(hm <sup>2</sup> ))		~17.9
Thermal bridges	y = 0.05 (W/m <sup>2</sup> K)		11.6
Total HTC			~81 W/K

Table 2: Summary of simulated test dwelling

Floor area	42.4 m <sup>2</sup>
Gross floor area	84.8 m <sup>2</sup>
Volume	210 m <sup>3</sup>
Envelope area	171 m <sup>2</sup>
Glazing Fraction	15.4 %
Glazing g-value	0.63
Heat loss parameter	0.96 W/Km <sup>2</sup>

### 248 3.3. Field tests

249 To support this simulated work, a number of results from  
 250 field tests are also presented. These include data from the NHBC  
 251 field trial (NHBC), described in Butler and Dengel [35], and  
 252 a number of tests performed under the Technology Strategy  
 253 Board Building Performance and Evaluation Programme [27],  
 254 therefore representing recently built, higher performance dwellings  
 255 - although not a representative sample. Anonymised summary  
 256 details of the case study tests used as part of this paper are pre-  
 257 sented in table A.10, All tests follow the basic method described  
 258 in section 2.1, with Case A1 and A2 representing repeat test pre  
 259 and post insulation.  
 260

## 261 4. Stored solar heat gains (SSHG)

262 An assumption of the steady state linear regression analysis  
 263 is that each data point is independent. However, the solar heat  
 264 absorbed on one day may be re-emitted by the thermal mass of  
 265 the dwelling across a period extending beyond the almost exclu-  
 266 sively used 24 hour aggregation interval (see table A.9). Figure  
 267 2 shows the response in electric heating power to the solar input  
 268 from a single day of the simulated test dwelling undergoing co-  
 269 heating. Here, the test dwelling is simulated under co-heating  
 270 conditions in a simplified weather file, in which  $T_e$  is held at  
 271 5°C and all other weather variables are set to zero or held con-  
 272 stant. Three cases are shown in which day 0 features a dull,

Table 3: Additional thermal mass cases - including thermal mass parameter (TMP)

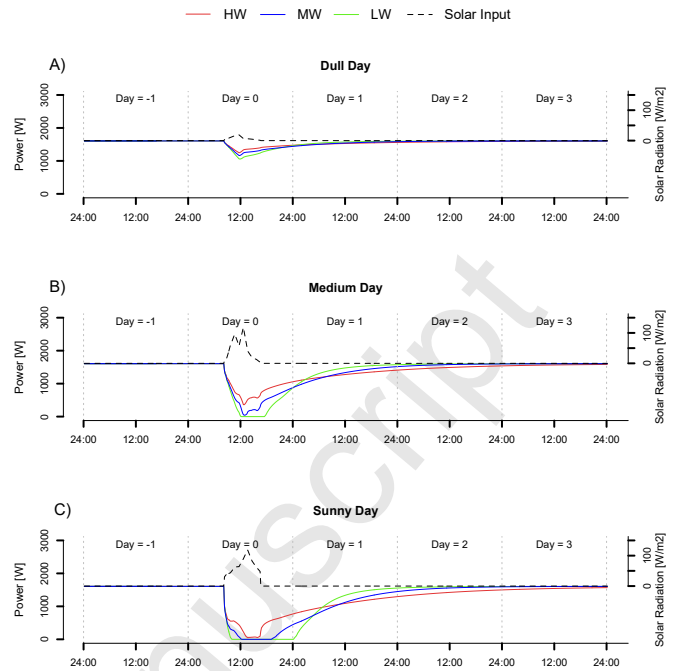
Case	External walls	Internal parti- tions	TMP (kJ/(m <sup>2</sup> K))
Heavyweight (HW)	Full fill mineral wool, brick & dense aggregate block	Dense blocks & plaster	470
Mediumweight (MW)	Full fill mineral wool, brick & aircrete block	Lightweight blocks & plaster	237
Lightweight (LW)	Timber frame, mineral wool, with brick outer leaf	Plasterboard on timber studs	99

Table 4: Additional glazing cases. Facade 1 is the South/East facade, whilst facade 2 is the North/West.

Case	Facade 1	Facade 2	Glazing frac- tion
Basecase	7.4 m <sup>2</sup>	5.6 m <sup>2</sup>	15.4%
Increased glazing	14.8 m <sup>2</sup>	5.6 m <sup>2</sup>	24.0%

medium or bright solar input. For each case, the thermal mass of the test dwelling is varied between light, medium and heavyweight cases. The electric heating response of the dwelling is then shown for the following 3 days, as well as the preceding day, describing how the heat input returns to the equilibrium state following the solar input. In this simplified scenario, it can clearly be seen that a fraction of the solar gains from a single days input can extend across multiple 24 hour aggregation periods, such that individual days can no longer be considered as fully independent.

A lightweight dwelling or lightweight elements will re-emit absorbed solar heat across a short time frame. This means that there will be a larger reduction in electric heating across the day of solar input with small contributions to subsequent days (figure 2). However, thermally massive elements or dwellings will only re-emit part of that stored solar heat within the same day as the solar input itself. This means a lower reduction in electric heating within the day of the solar input, but higher reductions across subsequent days or aggregation periods. Across periods of a few days, we should expect the total heat input from solar radiation to be the same in any case, according to laws of the conservation of energy. However, within daily aggregation periods there are distinct responses to solar inputs, and in heavyweight cases, a detachment between the measured solar input and the building's response - an effect that will impact the regression model which attempts to associate the two (see figure 3).

Figure 2: Building response to A) dull ( $0.4 \text{ kWhm}^{-2}\text{d}^{-1}$ ) B) medium ( $2.4 \text{ kWhm}^{-2}\text{d}^{-1}$ ) and C) sunny solar input ( $3.4 \text{ kWhm}^{-2}\text{d}^{-1}$ ) for three levels of thermal mass. Buildings are under steady state co-heating conditions with an internal temperature of  $25^\circ\text{C}$  and a constant external temperature of  $5^\circ\text{C}$ .

#### 4.1. Impact of SSHG upon HTC estimates

The impact of any stored solar heat gains upon HTC measurements is demonstrated within a Siviour plot<sup>2</sup> ( $Q_{elec}/\Delta T$  vs  $S/\Delta T$ ) of a simulated test, this time under a full weather file (figure 3). Here, the same 10 days are shown for a light, medium and heavyweight dwelling, again with the same  $H_{true}$  and otherwise identical. Corresponding data for the previous day's solar radiation ( $S_{t-1}$ ) is also plotted as a barplot at the base of the figure. What can be seen is that in duller days following sunny days, there is a tendency for heavyweight constructions to reduce their electric heating demand, as expected by our understanding of SSHG. On bright days, as seen earlier, lighter weight constructions are able to adsorb and re-emit a higher amount of solar radiation within the same day. This means that here the order is reversed and heavyweight dwellings require a higher amount of electric heating. The impact of both effects is to underestimate solar gains and to tend towards lower estimates of  $H_{meas}$  in heavyweight buildings - despite the fact this parameter is in fact identical in each case.

The full extent of this systematic bias depends upon further environmental conditions and both the order and the distribution of daily data points. For example, if a sunny day is followed by one of many dull days, then the influence of the biased data point may be small. However, in a pair of successive

<sup>2</sup>With the y-intercept indicating the HTC and the gradient of the best-fit line describing R.

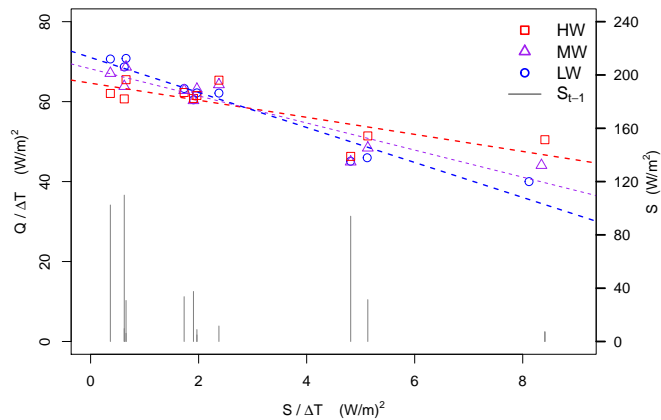


Figure 3: Siviour regression plot demonstrating the impact of thermal mass on daily data points and HTC estimates. The test dwelling has been simulated across 10 days using heavyweight (HW), mediumweight (MW) and lightweight (LW) constructions. The y-intercept represents the HTC and the gradient the value of the solar aperture,  $R$ . A 24:00-24:00 aggregation interval has been used.

and isolated sunny days, the biased data point will provide significant leverage and influence over the estimated HTC. Such factors mean it is worth examining the data and statistical influence of each data point [31] and also supports the benefit of a number of successive dull days within the test data [23, 51].

Nevertheless, the overall trend is for heavyweight buildings to underestimate the value of  $H_{true}$ . In figure 3,  $H_{true} = 75.1$  W/K, whilst the light, medium and heavyweight dwellings have measured values of 71.0, 68.2 and 64.6 W/K respectively. At the same time, the estimated solar aperture decreases from  $4.4 \text{ m}^2$  to  $3.4 \text{ m}^2$  and subsequently  $2.1 \text{ m}^2$  in the heavyweight case, as the amount of gains received and re-emitted within a single day decreases with thermal mass. Clearly, under this model and analysis framework, the value of  $R$  is a function of not only glazing characteristics of the dwelling but its thermal mass. This results in a complex and difficult to interpret parameter.

This tendency to underestimate results is demonstrated across a longer period in figure 4. Here, the test building is simulated in a series of two-week co-heating tests between October and March. With other building parameters held constant, the thermal mass of the test dwelling is again increased. What can be seen is that as the thermal mass increases, and SSHG increase, the underestimate of  $H_{true}$  also increases. A further mediumweight case is also plotted (MW - inc glazing) in which the south-facing glazing is doubled ( $14.8 \text{ m}^2$ ) whilst the overall HTC is maintained. Here, the underestimate bias again increases more significantly. This relationship between SSHG and underestimated HTCs is therefore both a function of the external environment as well as the glazing and mass characteristics of the test dwelling. This underestimating effect can help explain previously seen seasonal trends in repeated tests [23]

and underestimates in highly insulated dwellings [46].

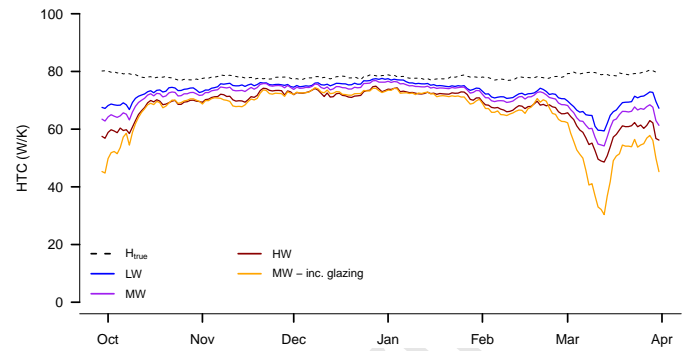


Figure 4: SSHG in full building contributions. The underestimate of  $H_{true}$  is seen to increase with higher thermal mass. Associated thermal mass parameters: LW = 99, MW = 237, HW =  $470 \text{ kJ/m}^2 \text{ K}$ . Note data from simulations is analysed in 2 week segments running from day 1 to day 14, then day 2 to 15 and so on.

#### 4.2. Limits upon testing

In figure 4, more extreme underestimates are seen in both October and March, as the weather becomes both warmer and sunnier. When solar gains offset total heat losses, the internal temperature will rise above the experimental set point. Initially, this will be for a few hours, following midday peaks in solar radiation, but will extend to last across aggregation intervals. During such periods, the dynamic heat flows within the test dwelling will significantly increase and steady state analysis is no longer viable. This particularly impacts the application of the co-heating method to highly glazed, well insulated dwellings (e.g. Passivhaus). Experimental solutions, such as applying external shading and elevated internal temperatures [35], may help increase the range of testing conditions but not without also altering the expected heat loss [31].

#### 4.3. Aggregation intervals

Everett [23] suggested dawn-to-dawn aggregation intervals were adopted, although this is not consistently adopted [47, Table A.9], with Butler and Dengel [35] concluding clarity is needed. Figure 5 shows the results seen in figure 4 for a heavyweight construction, analysed across five different aggregation intervals. Here the underestimate bias is seen to vary considerably with the interval used. The underestimate decreases in intervals that better associate the measured solar radiation with the lagged gains they provide across a single aggregation period, with a dynamic dawn-dawn aggregation providing the most accurate results in figure 5. However, as can be seen in figure 5, a 12:00-12:00 is preferable to 06:00-06:00 aggregation. Here, the first few hours of solar radiation are less significant than the additional hours of re-emitted heat within the tail. This means that in many cases the optimum aggregation interval lies sometime after dawn. However, in field tests, this optimum will prove difficult to determine and may introduce a degree of arbitrariness into the analysis, as it is likely to change dependent

upon the solar profile experienced during testing and the unknown thermal mass response of the test dwelling. Therefore, it is recommended that a dawn-dawn interval is used consistently to analyse such data. Importantly, assessing test data in such a manner can help identify the presence of any SSHG and bias.

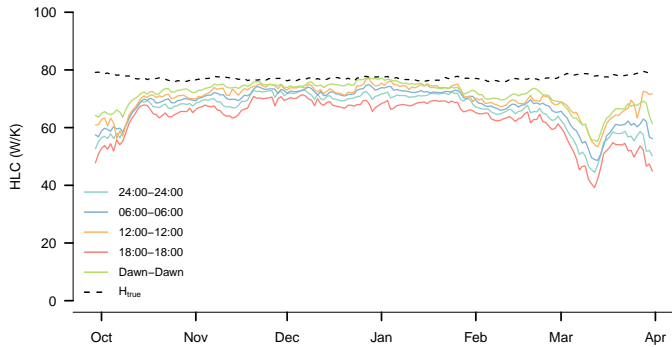


Figure 5: Reducing underestimate from stored solar contributions due to various aggregation intervals. Heavyweight test dwelling.

#### 4.4. Aggregation lengths

Alternatively, the aggregation length can be increased to capture a higher proportion of the lagged solar gains. The weakness of this approach is that the number of data points is reduced. In the previous case (figure 5), a 2-day aggregation length may be preferable to 1 day aggregations in modern, airtight dwellings (see table 5 where the root mean squared error (RMSE) of the various aggregation lengths are compared). However, in buildings where SSHG are less significant and there are large daily random errors (e.g. wind driven infiltration), then the advantage of two-day aggregations in handling SSHG is outweighed by the benefit of an increased number of data points [31]. The impact of increased aggregation lengths are also then reduced when appropriate intervals are used.

Table 5: Root mean square error across various aggregation lengths.

Aggregation Length	1 day	2 day	3 day
RMSE	8.0 W/K	6.2 W/K	8.3 W/K

#### 4.5. Field test data

Identifying systemic uncertainties within field tests can be extremely difficult. One such approach is to alter the analysis to highlight any discrepancies - here the aggregation interval. Table 6 shows eight field tests analysed across four different aggregation intervals. Here, in six of the eight cases, the highest HTC estimates are estimated with 06:00-06:00 or 12:00-12:00 aggregations, with 18:00-18:00 aggregations resulting in the lowest estimate in all these cases. Table 7 shows the results of seven tests performed on two paired test houses as part of the NHBC field trial. Again, six of the seven tests show their lowest HTC estimate during the 18:00-18:00 interval. There is also a trend for lower HTC estimates moving from colder and duller

conditions to warmer, sunnier periods. This would indicate the presence of SSHG and potential bias in HTC estimates - bias that is likely to reduce with appropriate aggregation intervals. It is therefore suggested that not only is data analysed on a dawn-to-dawn basis, but that data is examined across varying aggregation intervals to determine the likely presence of SSHG and bias. Incorporating this bias into uncertainty estimates is likely to be challenging, as it requires an understanding of the thermal response of the building to the solar radiation experienced during the test. Estimates of the associated uncertainty could be made based upon set bounds for the mass of the dwelling (type B uncertainty analysis) or by examining the range in HTC produced by different aggregation intervals.

Table 6: Field test results across four aggregation intervals. The difference between the HTC calculated at 06:00-06:00 and 18:00-18:00 aggregations is shown in the final column, in both absolute and relative terms.

Aggregation Interval	HTC (W/K)				Difference (W/K)
	24:00 - 24:00	06:00 - 06:00	12:00 - 12:00	18:00 - 18:00	
Case A1	245.0	247.2	241.7	240.5	6.7 (-3%)
Case A2	143.3	144.7	144.1	142.7	2.0 (-1%)
Case B	243.0	244.1	243.7	241.0	3.1 (-1%)
Case C	55.9	59.0	60.4	52.8	6.2 (-11%)
Case D	125.4	124.2	124.1	127.4	3.2 (+3%)
Case E	108.1	108.4	113.7	100.5	7.9 (-7%)
Case F	149.0	149.1	148.5	148.1	1 (-1%)
Case G	127.0	126.8	125.9	125.9	0.9 (-1%)

## 5. Measuring solar radiation

As discussed within section 2.2, there are two dominant forms of solar radiation measurements used within co-heating tests. Solar radiation is typically measured either vertically, in the plane expecting the highest amount of gains (e.g. south ( $S_{GVS}$ )), or a horizontal measurement is made ( $S_{GHR}$ ). The two are however not equivalent and do not provide equivalent results. A vertical measurement is likely to show a higher correlation to direct solar radiation at specific orientations, whilst the horizontal measurement will show higher correlation with diffuse gains, and a balanced value across all orientations.

When used in regression analysis, the two forms of solar radiation can therefore provide very different results. Figure 6 shows the test building simulated under co-heating conditions between October and March. The same building is then rotated by 90 degrees, such that it lies on an east-west axis, in figure 9. The impact of this change on the appropriateness of forms of solar measurements and on systemic error are discussed in the following two sections.

### 5.1. North-South orientated house

In the North-South case (figure 6), a vertically orientated south-facing measurement ( $S_{GVS}$ ) or vertical weighted mean ( $S_{GVWM}$ ) provide the most accurate  $H_{meas}$ , whilst a horizontal measurement ( $S_{GHR}$ ) overestimates  $H_{true}$ . The mechanics behind this effect are perhaps clearest when analysis using  $S_{GVS}$  and  $S_{GHR}$  are compared on the same plot. In the Siviour plot

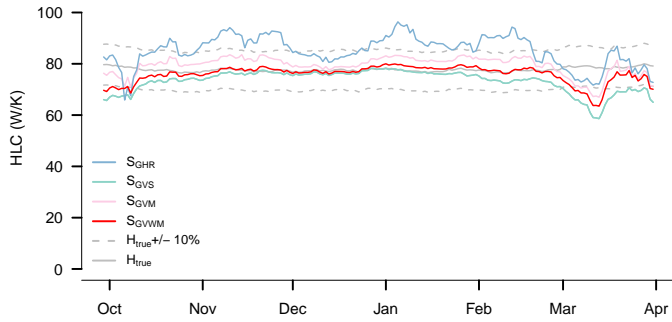


Figure 6: Derived HTC using a variety of measured solar radiations, south-north orientated dwelling.

ation.

487

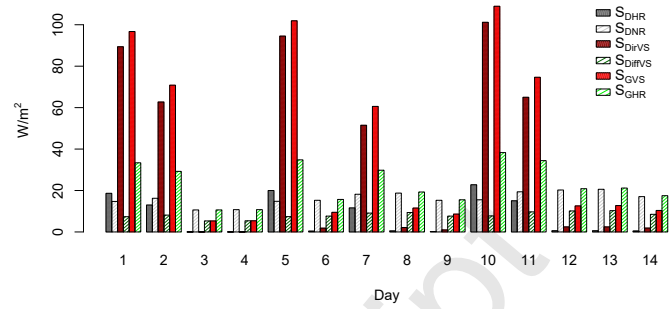


Figure 8: Respective solar characteristics for days in figure 7.

463 in figure 7, the same 2 week sample of data is plotted using  
 464 both  $S_{GHR}$  and  $S_{GVS}$ . Two distinct groups of data can be per-  
 465 ceived within both data sets, noting that it is only the measured  
 466 form of  $S$  that is changing between the two. Approximately  
 467 half the days, which appear dull, show similar distributions in  
 468 both data sets. However, a second group, with their individ-  
 469 ual days labeled in the plot, show distinct differences between  
 470 the two forms of measurement. This is made clear in figure 8,  
 471 where the vertical solar measurement captures the increase in  
 472 direct solar radiation on these days, whereas a horizontal mea-  
 473 surement does not. The horizontal measurement is unable to  
 474 sufficiently distinguish between days with low or high direct  
 475 gains, therefore higher solar gains are assumed across all days,  
 476 including the overcast mainly diffuse days, and an overestimate  
 477 of the HTC occurs.

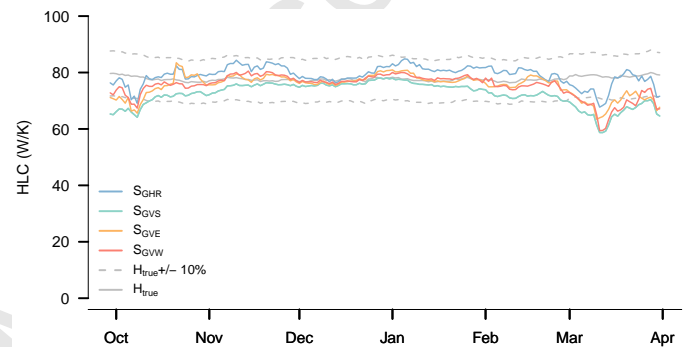


Figure 9: Derived HTC using a variety of measured solar radiations, east-west orientated dwelling.

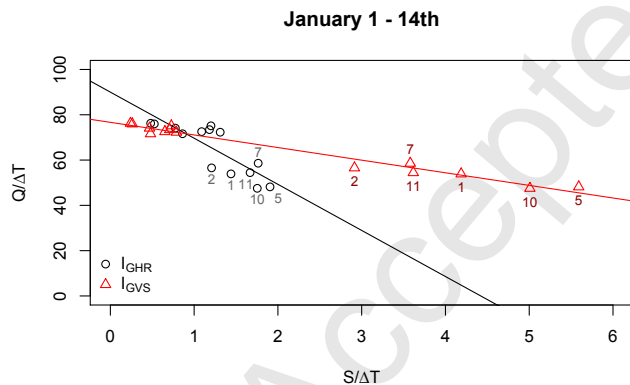


Figure 7: Siviour plot comparing analysis using  $S_{GHR}$  and  $S_{GVS}$ . Relevant days to figure 8 are labeled.

478 In summary, a horizontal measurement of solar radiation  
 479 is likely to provide significant bias in test dwellings receiving  
 480 significant direct gains into vertical openings. Vertical south-  
 481 facing or weighted means provide more accurate results, al-  
 482 though the later may require more complex measurements and  
 483 knowledge of the proportions of received solar radiation and  
 484 glazing characteristics across each facade. Finally, during some  
 485 periods, the overestimate caused by using a horizontal mea-  
 486 surement is countered by the underestimate from stored solar radi-

## 5.2. East-West orientated house

488

In an East-West orientated dwelling, there is no such domi-  
 489 nant facade and gains are split more evenly between direct and  
 490 diffuse components. The implications of this are:  
 491

- As direct gains are reduced,  $S_{GHR}$ , shows improved cor-  
 492 relation with the actual solar gains, now better represent-  
 493 ing the system and providing more accurate HTC esti-  
 494 mates.  
 495
- Vertical measurements in the plane of glazing ( $S_{GVE}$  or  
 496  $S_{GVW}$ ) provide improved HTC estimates in comparison  
 497 to a south-facing or horizontal measurements.  
 498
- In the example shown, east facing solar radiation mea-  
 499 surements (with  $7.4 \text{ m}^2$  of east facing glazing) provide  
 500 marginally improved results to a west orientation with  
 501 less glazing ( $5.7 \text{ m}^2$ ).  
 502

In any case, it would appear a vertical measurement is prefer-  
 503 able, in the plane of the dominant gains facade. In dwellings  
 504 with high proportions of glazing split across two equally domi-  
 505 nant facades, more accurate measurements may be obtained  
 506 from averaging vertical measurements from both orientations,  
 507 although in most cases a single measurement will suffice un-  
 508 less there is local shading effects. Mean vertical, or weighted  
 509

means, may provide more accurate results but this is dependent upon the proportion of diffuse to direct gains and distribution of glazing [31]. Finally, it should be noted the use of multiple solar measurements as separate regression variables is limited by the likely collinearity of the variables [47, 42, 31].

### 5.3. Field test results

On a limited number of occasions, field measurements have had access to both  $S_{GHR}$  and  $S_{GVS}$ . This was for repeated tests on Case A, a northeast - southwest ( $9 \text{ m}^2$  -  $5.7 \text{ m}^2$  respective glazed areas) orientated dwelling and a number of periods within the NHBC field trial [35], allowing the evaluation of the two test houses.

In the Case A test, there is negligible difference between the two measured solar approaches, although the entire test period was largely overcast and solar gains are estimated to be a very small percentage of  $Q_{elec}$  (4%). However, in the February NHBC tests,  $S_{GHR}$  produces a marginally higher HTC ( $\sim 3\text{-}4 \text{ W/K}$ ,  $Q_{sol} = 14\%$ ), an offset that increases ( $\sim 20\text{-}23 \text{ W/K}$ ) in tests performed in a significantly sunnier March period ( $Q_{sol} = \sim 30\text{-}40\%$ ).

Clearly, field test results under sunny conditions are sensitive to the form of solar radiation measurement made. The type of measurement required to avoid significant bias in results is dependent upon the test dwelling and the distribution of its glazing. In the majority of cases, on-site vertical measurements in the dominant or one of two dominant facades is likely to suffice. However, horizontal measurements risk bias and this may prohibit the use of more widely available meteorological measurements when using solar radiation in building energy models. Finally, consistent or equivalent measurements are vital to avoid error in comparisons or repeated measurements.

## 6. Conclusions

The ability to measure conventional buildings in the field remains crucial to providing control and understanding over the thermal performance of new builds and existing dwellings. However, to do so, testing must take place within the external environment. Therefore, the impact of the environment upon heat loss measurements, particularly from the presence of solar radiation, must be assessed. Through simulated and field co-heating tests this paper has highlighted two significant sources of uncertainty associated with solar radiation. Specifically, intrinsic uncertainty has been shown to be associated with the stored solar heat gains within a steady state approach:

- Fractions of solar gains received on one day can be re-emitted on subsequent days. As this heat flow is not captured in steady state analysis, an underestimate of the HTC can occur.
- This underestimate is more likely and more significant in heavyweight dwellings and those that admit more solar radiation into the internal space, e.g. highly glazed.

- Aggregating data from dawn-dawn will help reduce any underestimate. Additionally, comparing various aggregation periods may help identify the presence of stored solar heat.
- When internal temperatures rise significantly above the experimental set point, dynamic heat flows are increased and the steady state method is no longer valid. Solar gains and this experimental overheating provide the strongest limits on when testing can be performed in modern dwellings.

Further, the form of measured solar radiation has been shown to introduce bias even in otherwise ideal conditions. Any measurement of solar radiation will only be an imperfect representation of the complex distribution of S and solar gains across the building fabric, specifically:

- If a dwelling has the majority of its glazing, and therefore predicted solar gains, on the south facade, then a single south-facing vertical solar measurement is likely to give the most accurate HTC estimates.
- When the glazing and gains are split around a dwelling, e.g. east and west glazed facades, the choice of measured solar radiation is more complex. A mean vertical measurement,  $S_{GVM}$ , is likely to give the most accurate result. If only a single measurement is possible, then vertical measurement of the principal gains facade is likely to produce the most accurate results.
- Significantly, if a horizontal measurement of S is used for a building receiving predominantly direct gains, then a significant overestimate of the HTC can be retrieved, even in otherwise ideal conditions.

This paper has focused on the steady state co-heating method. However, the conclusions are likely to apply to different methods of characterising the thermal performance of buildings. For example, short term tests or overnight tests [21, 52, 53] need to ensure the thermal history of the building prior to testing or analysis is accounted for to avoid underestimates of heat loss through SSHG. Alternative approaches using smart metered data across longer, occupied periods, need to understand both the limits of ignoring solar gains, but also the dangers of utilising the commonly available horizontal solar radiation measurement and the artificial bias this may provide to heat loss estimates.

## Acknowledgments

This research was made possible by support from the EP-SRC Centre for Doctoral Training in Energy Demand (LoLo), grant numbers EP/L01517X/1 and EP/H009612/1. For secondary data used within the analysis, the authors are grateful to the NHBC and participants of the NHBC co-heating field trial: BRE, BSRIA, STROMA, Cardiff University Welsh School of Architecture, Loughborough University, Nottingham University and also to Leeds Beckett University.

## References

- 611 [1] B. Bordass, A. Leaman, and P. Ruysevelt. Assessing building performance in use 5: conclusions and implications. *Building Research & Information*, 29(2):144–157, 2001.
- 612 [2] ZCH. Closing the gap between design & as-built performance - evidence review report. Technical report, Zero Carbon Hub, London, UK, 2014.
- 613 [3] A. Stafford, M. Bell, and C. Gorse. Building confidence - a working paper. Technical report, Leeds Metropolitan University, Leeds, UK, 2012.
- 614 [4] GHA. Gha monitoring programme 2009-11: Technical report, results from phase 1: Post-construction testing of a sample of highly sustainable new homes. Technical report, Good Homes Alliance, 2011.
- 615 [5] J. Siviour. Experimental u-values of some house walls. *Building Services Engineering Research and Technology*, 15,1, 1994.
- 616 [6] S. Doran. Detr framework project report: Field investigations of the thermal performance of construction elements as built. Technical report, Building Research Establishment, Glasgow, UK, 2001.
- 617 [7] D. Johnston, D. Miles-Shenton, and D. Farmer. Quantifying the domestic building fabric ‘performance gap’. *Building Services Engineering Research and Technology*, 36(5):614–622, 2015.
- 618 [8] R.J. Lowe, J. Wingfield, M. Bell, and J.M. Bell. Evidence for heat losses via party wall cavities in masonry construction. *Building Services Engineering Research and Technology*, 28,2:161–181, 2007.
- 619 [9] H. Hens, W. Janssens, J. Depraetere, J. Carmeliet, and J Lecompte. Brick cavity walls: A performance analysis based on measurements and simulations. *Journal of Building Physics*, 31,2:96–124, 2007.
- 620 [10] C. Bankvall. Forced convection. practical thermal conductivity in an insulated structure under the influence from workmanship and wind. *ASTM symposium on Advances in Heat Transmission Measurement on Thermal Insulation Material Systems*, 1977.
- 621 [11] C. Rye. The spab research report 1. u-value report. Technical report, SPAB - Society for the Protection of Ancient Buildings, Glasgow, UK, 2010.
- 622 [12] P. Baker. Historic scotland technical paper 10 - u-values and traditional buildings. Technical report, Historic Scotland & Glasgow Caledonian University, 2011.
- 623 [13] S. Birchall. Co-heating tests - what and how? In *52nd Annual General Meeting (AGM) for BSRIA, The Building Services Research and Information Association*, London, 13th October 2011, 2011.
- 624 [14] FGN. Li, A. Smith, P. Biddulph, I.G Hamilton, R. Lowe, A. Mavrogiani, E. Oikonomou, R. Raslan, S. Stamp, A. Stone, A. Summerfield, D. Veitch, V. Gori, and T. Oreszczyn. Solid-wall u-values: heat flux measurements compared with standard assumptions. *Building Research & Information*, 43,2:238–252, 2014.
- 625 [15] ZCH. Closing the gap between design & as-built performance - interim progress report. Technical report, Zero Carbon Hub, London, UK, 2013.
- 626 [16] ISO 13790:2008. Bs en iso 13790:2008 energy performance of buildings - calculation of energy use for space heating and cooling. Technical report, International Organization for Standardization (ISO), Geneva, Switzerland, 2008.
- 627 [17] C. Roulet and F. Foradini. Simple and cheap air change rate measurement using co2 concentration decays. *International Journal Of Ventilation*, 1(1):39–44, 2006.
- 628 [18] ISO9869:2014. Bs en iso 9869:2014 thermal insulation: Building elements: In-situ measurement of thermal resistance and thermal transmittance. Technical report, International Organization for Standardization (ISO), Geneva, Switzerland, 2014.
- 629 [19] R.C. Sonderegger and M. Modera. Electric co-heating: A method for evaluating seasonal heating efficiencies and heat loss rates in dwellings. *Second CIB Symposium on Energy Conservation in the Built Environment, Copenhagen, Denmark, May 28th - June 1st, 1979*, 1979.
- 630 [20] R.C. Sonderreger, P. Condon, and M. Modera. In-situ measurement of residential energy performance using electric coheating. *American Society of Heating, Refrigerating and Air Conditioning Engineers Transactions*, 86:394, 1980.
- 631 [21] K. Subbarao. Pstar -primary and secondary terms analysis and renormalization: A unified approach to building energy simulations and short - term monitoring. Technical report, Solar Energy Research Institute, Golden, Colorado, US, 1988.
- 632 [22] J.B. Siviour. Experimental thermal calibration of houses. *Conference on Comparative Experimentation of Low Energy Houses*, 1981.
- 633 [23] R. Everett. Rapid thermal calibration of houses. Technical report, Science and Engineering Research Council, 1985.
- 634 [24] M. Bell and R.J. Lowe. The york energy demonstration project, final report. Technical report, Leeds Metropolitan University, Leeds, UK, 1998.
- 635 [25] J. Wingfield, M. Bell, D. Miles-Shenton, and J. Seavers. Elm tree mews field trial - evaluation and monitoring of dwellings performance final technical report. Technical report, Leeds Metropolitan University, Leeds, UK, 2011.
- 636 [26] D. Miles-Shenton, J. Wingfield, R. Sutton, and M. Bell. Project title: Temple avenue project, part 1: Temple avenue field trial - evaluation of design & construction process and measurement of fabric performance of new build dwellings part 2: Energy efficient renovation of an existing dwelling: Evaluation of design & construction and measurement of fabric performance. Technical report, Leeds Metropolitan University, Leeds, UK, 2011.
- 637 [27] J. Palmer, D. Godoy-Shimizu, A. Tillson, and I. Mawditt. Building performance evaluation programme: Findings from domestic projects - making reality match design. Technical report, Innovate UK, North Star House, North Star Avenue, Swindon, UK, 2016.
- 638 [28] J. Wingfield. In-situ measurement of whole house heat loss using electric coheating. Technical report, Leeds Metropolitan University, Leeds, UK, 2010.
- 639 [29] GHA. Detailed description of coheating test procedure - indicative example. Technical report, Good Homes Alliance & Leeds Metropolitan University, 2011.
- 640 [30] D. Johnston, D. Miles-Shenton, D. Farmer, and J. Wingfield. Whole house heat loss test method (coheating). *IEA Annex 58: Reliable Building Energy Performance Characterisation Based on Full Scale Dynamic Measurements, 2nd Meeting, April 2nd - 5th, Bilbao, Spain, 2012*, 2012.
- 641 [31] S. Stamp. *Assessing uncertainty in co-heating tests: Calibrating a whole building steady state heat loss measurement method*. PhD thesis, University College London, September 2015.
- 642 [32] L.S. et al. Palmiter. Low cost performance evaluation of passive solar buildings. Technical report, Solar Energy Research Institute, Golden, Colorado, US, 1979.
- 643 [33] G. Bauwens, P. Standaert, S. Roels, and F. Delcuve. Reliability of co-heating measurements. *IEA Annex 58: Reliable Building Energy Performance Characterisation Based on Full Scale Dynamic Measurements, 2nd Meeting, April 2nd - 5th, Bilbao, Spain, 2012*, 2011.
- 644 [34] P. Baker. A retrofit of a victorian terrace house in new bolsover: A whole house thermal performance assessment. Technical report, Historic England & Glasgow Caledonian University, 2015.
- 645 [35] D. Butler and A. Dengel. Review of co-heating test methodologies. Technical report, NHBC Foundation, London, UK, 2013.
- 646 [36] ZCH. Closing the gap between design & as-built performance - end of term report. Technical report, Zero Carbon Hub, London, UK, 2014.
- 647 [37] P.H. Baker and H.A.L. van Dijk. Paslink and dynamic outdoor testing of building components. *Building and Environment*, 43:143–151, 2008.
- 648 [38] S. Stamp, R. Lowe, and H. Altamirano-Medina. An investigation into the role of thermal mass on the accuracy of co-heating tests through simulations & field results. In *Building Simulation and Optimization 2013*, Chambéry, France, August 25-28, 2013.
- 649 [39] S. Stamp, R. Lowe, and H. Altamirano-Medina. Solar driven uncertainty in co-heating. In *IEA Annex 58: Reliable Building Energy Performance Characterisation Based on Full Scale Dynamic Measurements*, 4th Meeting, April 8th - 10th, Holzenkirchen, Germany, 2013, 2013.
- 650 [40] D. Johnston, D. Miles-Shenton, D. Farmer, and J. Wingfield. Whole house heat loss test method (coheating). Technical report, Leeds Metropolitan University, Leeds, UK, 2013.
- 651 [41] BRE. Sap 2012 - the government’s standard assessment procedure for energy rating of dwellings - 2012 edition. Technical report, Building Research Establishment, Garston, Watford, 2014.
- 652 [42] G. Bauwens and S. Roels. Co-heating test: A state-of-the-art. *Energy & Buildings*, 82:163–172, 2014.
- 653 [43] JCGM. Evaluation of measurement data - guide to the expression of uncertainty in measurement. Technical report, Joint Committee for Guides in Metrology (JCGM/WG1), 2008.
- 654 [44] LBNL. Energyplus engineering reference - the reference to energyplus calculations. Technical report, University of Illinois Urbana-Champaign, Lawrence Berkeley National Laboratory, 2014.
- 655 [45] S. Stamp, R. Lowe, and H. Altamirano-Medina. Using simulated co-

## Appendix A. Appendix

- 752 heating tests to understand weather driven sources of uncertainty within  
 753 the co-heating test method. In *ECEEE Summer Study Proceedings*, pages  
 754 2049–2055, Presqu'île de Giens, Toulon/Hyeres, France, June 3-8, 2013.
- 755 [46] D.K. Alexander and H.G. Jenkins. The validity and reliability of co-  
 756 heating tests made on highly insulated dwellings. In *Energy Procedia*,  
 757 *6th International Building Physics Conference, IBPC 2015*, pages 1732–  
 758 1737, 2015.
- 759 [47] A.H. Deconinck and K. Leunis. Co-heating: a critical evaluation of data  
 760 analysis methods. Masters thesis, Katholieke Universiteit Leuven, 2012.
- 761 [48] G. Bauwens, P. Standaert, S. Roels, and F. Delcuve. Reliability of co-  
 762 heating measurements. In *First Building Simulation and Optimization*  
 763 *Conference*, pages 348–355, Loughborough, UK 10-11 September, 2012,  
 764 2012.
- 765 [49] ISO13770:2007. Bs en iso 13370: 2007 - thermal performance of build-  
 766 ings – heat transfer via the ground – calculation methods. Techni-  
 767 cal report, International Organization for Standardization (ISO), Geneva,  
 768 Switzerland, 2007.
- 769 [50] DCLG. The building regulations 2010 - conservation of fuel and power -  
 770 approved document 11a - conservation of fuel and power in new dwellings  
 771 - 2013 edition. Technical report, Department of Communities and Local  
 772 Government, 2013.
- 773 [51] R. Lowe and C. Gibbons. Passive solar houses: Availability of weather  
 774 suitable for calibration in the uk. *Building Services Engineering Research*  
 775 *and Technology*, 9,3:127–132, 1988.
- 776 [52] E. Mangematin, G. Pandraud, and D. Roux. Quick measurements of  
 777 energy efficiency of buildings. *Comptes Rendus Physique*, 13:383–390,  
 778 2012.
- 779 [53] G. Pandraud and R. Fitton. Qub: Validation of a rapid energy diagnostic  
 780 method for buildings. In *IEA Annex 58: Reliable Building Energy Per-*  
 781 *formance Characterisation Based on Full Scale Dynamic Measurements,*  
 782 *4th Meeting, April 8th - 10th, Holzenkirchen, Germany, 2013*, 2013.
- 783 [54] F. Stevenson and H. Rijal. Paper no 595: The sigma home: towards an  
 784 authentic evaluation of a prototype building. In *PLEA 2008 ? 25th Con-*  
 785 *ference on Passive and Low Energy Architecture, 22nd to 24th October*  
 786 *2008*, Dublin, Rep. of Ireland, 2008.
- 787 [55] J. Wingfield, M. Bell, D. Miles-Shenton, R. Lowe, and T. South. Evalu-  
 788 ating the impact of an enhanced energy performance standard on load-  
 789 bearing masonry domestic construction, report number 8 - final re-  
 790 port, lessons from stamford brook understanding the gap between de-  
 791 signed and real performance. Technical report, Department for Commu-  
 792 nities and Local Government, AECOM, Leeds Metropolitan University,  
 793 Leeds, UK, 2007.
- 794 [56] M. Siddal, J. Trinick, and D. Johnston. Testing the real heat loss of a  
 795 passivhaus building: Can the uk's energy performance gap be bridged?  
 796 In *Proceedings of the 17th International Passivhaus Conference 2013,*  
 797 *19-20th April 2013*, pages 159 –166, Congress Center Messe Frankfurt,  
 798 Frankfurt, Germany, 2013.
- 799 [57] Innovate UK. Building performance evaluation: Avante homes - fabric  
 800 performance and occupancy feedback. Technical report, Innovate UK,  
 801 North Star House, North Star Avenue, Swindon, UK, 2016.
- 802 [58] Innovate UK. Building performance evaluation: Passivhaus bungalow  
 803 development, houghton-le-spring. Technical report, Innovate UK, North  
 804 Star House, North Star Avenue, Swindon, UK, 2016.
- 805 [59] Innovate UK. Building performance evaluation: The old applestore,  
 806 stawell. Technical report, Innovate UK, North Star House, North Star  
 807 Avenue, Swindon, UK, 2016.
- 808 [60] Innovate UK. Building performance evaluation: Building performance of  
 809 high density apartments - andre street, london. Technical report, Innovate  
 810 UK, North Star House, North Star Avenue, Swindon, UK, 2016.
- 811 [61] Innovate UK. Building performance evaluation: Cross lane development,  
 812 barnsley. Technical report, Innovate UK, North Star House, North Star  
 813 Avenue, Swindon, UK, 2016.
- 814 [62] Innovate UK. Building performance evaluation: Advanced control on  
 815 code 4 properties with heat pumps. Technical report, Innovate UK, North  
 816 Star House, North Star Avenue, Swindon, UK, 2016.
- 817 [63] Innovate UK. Building performance evaluation: Bloom court. Technical  
 818 report, Innovate UK, North Star House, North Star Avenue, Swindon,  
 819 UK, 2016.
- 820 [64] Innovate UK. Building performance evaluation: Code level 5 homes -  
 821 lyndhurst crescent, swindon. Technical report, Innovate UK, North Star  
 822 House, North Star Avenue, Swindon, UK, 2016.

Table 7: Field test results across four aggregation intervals. Paired test houses (control A and test B) tested between Dec-Apr.

Aggregation Interval	HTC (W/K)				Difference (W/K)	Mean S (W/m <sup>2</sup> )	$T_e$ (°C)
	24:00 - 24:00	06:00 - 06:00	12:00 - 12:00	18:00 - 18:00			
Dec/Jan - A	77.1	77.0	78.6	74.5	2.5 (-3%)	26.7	6.6
Dec/Jan - B	77.2	75.0	74.0	76.3	1.3 (+2%)	26.7	8.7
Jan/Feb - A	66.1	70.1	69.5	59.4	10.7 (-15%)	64.2	4.6
Jan/Feb - B	72.5	73.4	78.7	64.3	9.1 (-12%)	64.2	5.7
Feb - B	67.4	71.1	74.8	64.3	6.8 (-10%)	62	5.7
Mar - B	61.4	63.2	66.2	58.2	5.1 (-8%)	132	8.1
Apr - B	61.6	62.7	63.4	58.9	3.8 (-6%)	123	8.7

Table 8: Comparison of types measured solar radiation on field HTC and R estimates. Uncertainty estimates for primary sources are calculated based on the JCGM 'Guide to the expression of uncertainty in measurement' [43]. Presented at 95% confidence intervals. Secondary data sources, indicated by a \*, are estimated from the standard error of regression (at 95% c.i.).

Test dwelling	Date	Measured S	HTC (W/K)	R (m <sup>2</sup> )	Mean S (± s.d.) (W/m <sup>2</sup> )	
Case A1	March	$S_{GHR}$	144 ± 12	2.6 ± 2.7	60 ± 26	
		$S_{GVS}$	144 ± 10	4.5 ± 2.9	37 ± 26	
NHBC	Test house	$S_{GHR}$	73 ± 8	3.8 ± 2.8	62 ± 24	
		$S_{GVSE}$	71 ± 6	2.7 ± 1.0	82 ± 55	
	Control house*	Feb	$S_{GHR}$	71 ± 10	4.6 ± 3.2	62 ± 24
			$S_{GVSE}$	68 ± 4	2.7 ± 0.8	82 ± 55
	Test house*	March	$S_{GHR}$	52 ± 16	1.1 ± 1.6	166 ± 35
			$S_{GVSE}$	44 ± 8	0.6 ± 1.6	95 ± 50
	Control house*	March	$S_{GHR}$	54 ± 12	2.2 ± 1.0	166 ± 35
			$S_{GVSE}$	31 ± 8	0.2 ± 1.6	95 ± 50

Table A.9: Details of reported field tests. NR = Not reported. Note: Both TSB and GHA programmes were conducted by various groups, ostensibly following the protocol provided by Leeds Beckett University, which recommended vertical south facing radiation [29, 28]. Evidence below suggests this was not consistently followed or adopted.

Case study	$H_{meas}$ (W/K)	Duration (Days)	Solar Measurement	Aggregation length	Aggregation Interval	Reference
Sigma house	144	NR	NR	NR	NR	[54]
Elm Tree Mews	136	11	$S_{GVS}$	24 hour	NR	[55]
Stamford Brook - A	112	11	$S_{GVS}$	24 hour	NR	[8]
Stamford Brook - B	153	22	$S_{GVS}$	24 hour	NR	[8]
<b>Good Homes Alliance Building Performance &amp; Evaluation Programme</b>						
GHA - A	150	32	NR	24 hour	NR	[4]
GHA - B	133	32	NR	24 hour	NR	"
GHA - C	110	18	NR	24 hour	NR	"
GHA - D	49	28	NR	24 hour	12am-12am & 6am-6am	"
<b>NHBC Field Trial</b>						
Participant A	64	NR	$S_{GHR}$	24 hour	NR	[35]
Participant B	65	10	NR	24 hour	NR	"
Participant C	70	13	$S_{GVS}$	24 hour	NR	"
Participant D	65/73	15	$S_{GVS}/S_{GHR}$	24 hour	NR	"
Participant E	61	14	$S_{GHR}$ converted to $S_{GVS}$	24 hour	NR	"
Participant F	57	13	$S_{GVS} + S_{GVN}$	24 hour	6pm-6pm	"
Participant G	74	13	$S_{GHR}$	24hour + Nighttime	NR	"
<b>TSB Building Performance &amp; Evaluation Programme</b>						
Ebbw Vale - Lime	45	18	NR	24 hour	12pm - 12pm	[56]
Ebbw Vale - Larch	150	15	NR	24 hour	12pm - 12pm	"
Avante housing	121.6	NR	$S_{GVS}$	24 hour	NR	[57]
Houghton-le-spring 1	46.7	NR	NR	24 hour	NR	[58]
Houghton-le-spring 2	38.1	NR	NR	24 hour	NR	"
Stawell	110.5	NR	$S_{GVS}$	24 hour	NR	[59]
Andre St. Plot 6	69.3	NR	None	24 hour	NR	[60]
Andre St. Plot 4	81.6	NR	None	24 hour	NR	"
Cross Lane	103.1	NR	$S_{GHR}$	24 hour	NR	[61]
Crarey/ Ratby	139.2	NR	Offsite	24 hour	NR	[62]
Crarey/ Ratby 2	101.7	NR	Offsite	24 hour	NR	"
Bloom Court	67.2	NR	NR	24 hour	NR	[63]
Lyndhurst? 1	93.8	NR	NR	24 hour	NR	[64]
Lyndhurst? 2	103.6	NR	NR	24 hour	NR	"

Table A.10: Summary of field tests used in analysis (\* Indicates secondary data source). Uncertainties for primary sources stated at 95% confidence intervals, based upon the Guide to Measurement Uncertainty [43], see [31].

Case	$H_{meas}(W/K)$	When	Duration	Solar Measurement	Dwelling Type	Wall construction	Floor Area	Orientation
NHBC	71±6	Feb	13 days	$S_{GHR}$ & $S_{GVSE}$	Detached	Brick-clad timber frame	84 m <sup>2</sup>	SSE
Case A1	245 ±21	Jan-Feb	26 days	$S_{GHR}$ & $S_{GVS}$	Semi-detached	Brick-cavity-block (un-insulated)	103 m <sup>2</sup>	SSW
Case A2	143±10	Mar-Apr	15 days	$S_{GVSSW}$	Semi-detached	Brick-polybead-block (insulated)	103 m <sup>2</sup>	SSW
Case B	231±21	Mar	15 days	$S_{GVSE}$	Detached	Thin joint masonry	192 m <sup>2</sup>	SE
Case C	56±16	Dec	6 days	$S_{GVSW}$	Detached	Timber frame, Passivhaus	99 m <sup>2</sup>	SW
Case D	135±19	Dec	17 days	$S_{GHR}$	Detached	Aircrete thin-joint	132 m <sup>2</sup>	E
Case E*	94	Feb	18 days	$S_{GHR}$	Semi-detached	Aerated clay blocks	84 m <sup>2</sup>	SSE
Case F*	149	Jan-Feb	22 days	$S_{GVS}$	Detached	Thin-joint masonry	151 m <sup>2</sup>	S
Case G*	133	Jan-Feb	22 days	$S_{GVS}$	Detached	SIP	154 m <sup>2</sup>	S